Author Manuscript

Author Manuscript

Author Manuscript

Author Manuscript

HHS Public Access

Author manuscript

Nature. Author manuscript; available in PMC 2009 May 20.

Published in final edited form as:

Nature. 2008 November 20; 456(7220): 413–416. doi:10.1038/nature07350.

The ion pathway through the opened Na+,K+-ATPase pump

Ayako Takeuchi, **Nicolás Reyes**, **Pablo Artigas**, and **David C. Gadsby**

Laboratory of Cardiac/Membrane Physiology, The Rockefeller University, New York, NY 10065, USA

Abstract

P-type ATPases pump ions across membranes, generating steep electrochemical gradients that are essential for the function of all cells. Access to the ion-binding sites within the pumps alternates between the two sides of the membrane1 to avoid the dissipation of the gradients that would occur during simultaneous access. In Na^+,K^+-ATPase pumps treated with the marine agent palytoxin, this strict alternation is disrupted and binding sites are sometimes simultaneously accessible from both membrane sides, transforming the pumps into ion channels (e.g., refs 2,3). Current recordings in these channels can monitor accessibility of introduced cysteine residues to water-soluble sulphydryl-specific reagents4. We found previously5 that Na^+,K^+ pump-channels open to the extracellular surface through a deep and wide vestibule that emanates from a narrower pathway between transmembrane helices TM4 and TM6. Here we report that cysteine scans from TM1 through TM6 reveal a single unbroken cation pathway that traverses palytoxin-bound Na^+,K^+ pump-channels from one side of the membrane to the other. This pathway comprises residues from TM1, TM2, TM4, and TM6, passes through ion-binding site II, and is likely conserved in structurally and evolutionarily related P-type pumps, such as SERCA- and H^+,K^+-ATPases.

The Na^+,K^+-ATPase is a P-type (named for its phosphorylated intermediate) pump that exports three Na^+ ions and imports two K^+ ions per ATP hydrolysed. The ion-binding sites are accessible from the extracellular space in the phosphorylated conformation, called E2P, and from the cytoplasm in the dephosphorylated configuration, E1. But the routes by which ions approach and leave those sites have remained elusive6 despite X-ray crystal structures of sarcoplasmic- and endoplasmic-reticulum Ca^{2+}-ATPase (SERCA) P-type pumps in several states6-11, although recently a BeF_3^--trapped E2P-like state captured an open luminal pathway12,13. However, sensitive electric current recording methods developed for studies of ion channels14 have begun to probe the ion pathway of the Na^+,K^+ pump 5,15-18, after its transformation into an ion channel by palytoxin2 and electrophysiological analyses of reactivity of introduced cysteines to methanethiosulphonate (MTS) reagents4.

Users may view, print, copy, and download text and data-mine the content in such documents, for the purposes of academic research, subject always to the full Conditions of use:http://www.nature.com/authors/editorial_policies/license.html#terms

Address for correspondence: David C. Gadsby, Laboratory of Cardiac/Membrane Physiology, Rockefeller University, 1230 York Avenue, New York, NY 10065, USA, E-mail: gadsby@rockefeller.edu, Tel: 212-327-8680, Fax: 212-327-7589.

Reprints and permissions information is available at www.nature.com/reprints.

The authors declare no competing financial interests.

Author Manuscript Author Manuscript Author Manuscript Author Manuscript

Cysteines modified by MTS reagents in palytoxin-bound Na^+,K^+ pump-channels include those substituted for ion-binding19-21 acidic residues in the pocket between transmembrane helices TM4 (e.g. E336, equivalent to SERCA E309) and TM6 (e.g. D813, equivalent to SERCA N796), as well as T806 (P789 in SERCA) at the outermost end of TM6 within the external vestibule floor5,16,17. These three positions approximately align (Fig 1) in extracellular views of the transmembrane domain of the Na^+,K^+-ATPase, whether of the recent21 E2·MgF_4^{2-} Na^+,K^+-ATPase structure (Fig 1a), an occluded conformation with both cytoplasmic and extracellular pathways shut, or of a model based on the E2P-like SERCA E2·BeF_3^- structure12,13 (Fig 1b), with cytoplasmic pathway shut but extra-cytoplasmic pathway open. However, palytoxin, with Na^+ and ATP present, appears to stabilize an E2P-related Na^+,K^+ pump conformation22,23 in which the gates to the binding sites can both be open3, a structure not yet visualized (nor expected) for any native P-type pump. In occluded structures of SERCA containing 2 Ca^{2+} ions7,10,11 and of Na^+,K^+-ATPase21 containing 2 K^+ ions, side chains of residues in TM5 and TM6 help coordinate the bound ion in site I, and TM4 and TM6 side chains help coordinate that in site II. The near alignment of accessible TM4 and TM6 positions (Fig. 1) therefore raises two questions: do ions in the Na^+,K^+ pump's extracellular pathway flow between TM4, TM6, and TM5 (ref. 17) or between TM4, TM6, TM2, and TM1 (cf. refs. 6,12,13) (Fig. 1; red question marks), and what pathway(s) do ions take from the binding sites to the cytoplasm?

To answer these questions, we first introduced cysteines, one at a time, at 20 contiguous positions (I778-I797) along TM5, and 4 more (A798-P801) in the external loop connecting TM5 and TM6, into the *Xenopus* Na^+,K^+-ATPase α1 subunit made ouabain resistant by the mutation24 C113Y. We coexpressed each cysteine-tagged mutant with the *Xenopus* β3 subunit in *Xenopus* oocytes5,18. After applying 50 nM palytoxin (Fig. 2a-d; black downward arrowheads) to outside-out membrane patches, to transform all Na^+,K^+ pumps into ion channels (signals from native ouabain-sensitive *Xenopus* Na^+,K^+ pumps were prevented by 100 μM ouabain in all external solutions), we assessed reactivity of positively-charged membrane-impermeant $MTSET^+$ (2-trimethylammonium-ethyl-methanethiosulphonate, 1 mM; blue arrows) with each engineered cysteine. Reaction was signalled by alteration of the inward Na current (symmetrical 125 mM [Na] solutions with -50 −mV membrane potential) flowing through pump-channels (Fig. 2). $MTSET^+$ tests were preceded by exposure to 10 mM dithiothreitol (grey arrows) to restore any spontaneously oxidised thiols. There was no evidence of $MTSET^+$ reaction with any residue in TM5, but it rapidly decreased current ∼25% in construct N799C with a cysteine in the TM5-TM6 loop (Fig. 2a).

We similarly scanned 21 contiguous positions (F99-I119) in TM1, 11 (Y133-V142, T145) in TM2, and 6 (Q120, Q128-L132) in the extracellular TM1-TM2 connecting loop, testing reactivity of each introduced cysteine with 1 mM $MTSET^+$ (Fig. 3). Reactive positions (defined as >10% change in pump-channel current) in TM1 were 100-103, 106, 113, 116 and 117 (Fig. 3a-c), in the TM1-TM2 loop included 120, 128, 130 and 131 (Fig. 3c,f), and in TM2 included 133 and 134 at the outer end and 145 towards the cytoplasmic end (Fig. 3d-f).

The summarized results from these scans, mapped onto an Na^+,K^+ pump homology model based on the SERCA E2·BeF_3^- structure, show as red sticks residues in positions where

Author Manuscript Author Manuscript Author Manuscript Author Manuscript

substituted cysteines showed evidence of modification by 1 mM $MTSET^+$, and as yellow sticks residues in positions where there was no evidence of reactivity (Fig. 4a,b). Our previously reported5 results on reactive cysteines introduced in TM4 (E321, E336, G337), TM5-TM6 loop (L802-L804) and TM6 (G805-C811, D813, D817) are included. To fill gaps, we tested 16 additional strategically-located positions in TM3 (I290, I294, I297, A301) and TM4 (A322-F325, I327, G328, V331, A332, P335, L339, T341, V342): only P335C and L339C mutants showed reactivity with $MTSET^+$.

The red residues mark out a single, unbroken $MTSET^+$-accessible pathway (Figs. 4a,b; Supplementary Figs. 1,2) that courses between TM1, TM2, TM6, and TM4, rather than between TM5, TM4, and TM6 (Fig. 4a; Supplementary Figs. 1,2), passes through site II, and spans the full distance across the membrane (approximate boundaries indicated by lines ∼35 Å apart in Fig. 4b; see also Supplementary Fig. 2 and movie). Red reactive positions are enveloped in a yellow non-responsive surround (Fig. 4a-b; Supplementary Fig. 2a-b), indicating that the scan was complete and so fully delimits this principal pathway through the pump. Moreover, as current was practically abolished after $MTSET^+$ modification of TM1 position 106 (Figs. 3a,c, 4c,d, and Supplementary Figs. 4a, 7c,g), or positions 337 in TM4 (ref. 5) or 806 in TM6 (ref. 5; Supplementary Fig. 3b), the pathway depicted in Fig. 4 (and Supplementary Fig. 2) is likely the sole route for rapid ($\sim 10^7\ s^{-1}$) Na^+-ion flow through palytoxin-bound Na^+,K^+ pump-channels.

The negative charges of site II residues E336 (TM4) and D813 (TM6), largely conserved in P-type cation pumps, form a cation-selectivity filter5. This was proposed responsible for the apparent lack of reactivity of a cysteine substituted for nearby G337 with negatively charged $MTSES^-$ (2-sulphonato-ethyl-methanethiosulphonate), despite reaction with similarly sized, but positively charged, $MTSET^+$ (ref. 5). $MTSET^+$ reaction with cysteines substituted for deeper TM1 residues L106, S103, F102, G101, and G100 (Fig. 4c) decreased current ∼40-90% (Figs. 3a-c and 4c,d). The smaller current decrease, 20-30%, on reaction with the comparably-sized neutral reagent MTSACE (2-aminocarbonyl-ethyl-methanethiosulphonate; Fig. 4c,e and Supplementary Fig. 4) is consistent with simple steric interference with Na^+ current flow by the ∼6-Å × 8-Å adduct. Negatively charged $MTSES^-$, however, failed to react, neither altering pump-channel current nor preventing its subsequent decrease by $MTSET^+$ (Fig. 4c and Supplementary Fig. 4a,c); deep TM2 position T145 (cf. Fig. 3f) behaved comparably. In contrast, $MTSES^-$ increased current in pump-channels with cysteines at more superficial TM1 position A116, and TM1-TM2 loop residues Q128 and D130 (as previously shown18 for Q120 and N131), the negative adduct electrostatically elevating the local concentration of current-carrying Na^+ ions5,18. These results show that MTS reagents had to pass the cation selectivity filter formed by E336 and D813 to reach every deeper reactive cysteine.

Our findings are all broadly consistent with corresponding locations of target residues in the Na^+,K^+ pump model based on the SERCA E2·BeF_3^- structure (Figs. 1b, 4a,b, and Supplementary Figs. 1,2), supporting its overall applicability. This is despite both the mere 26% amino acid identity between SERCA and Na^+,K^+-ATPase in the TM1-TM6 region scanned here, and the fact that the cytoplasmic-side pathway is tightly12,13 closed in SERCA E2·BeF_3^- (also, apparently, in Na^+,K^+-ATPase E2·BeF_3^-; Supplementary Fig. 5)

Author Manuscript Author Manuscript Author Manuscript Author Manuscript

whereas it can demonstrably open in the Na^+,K^+ pump-channel. That open cytoplasmic access pathway runs between TM1, TM2, and TM4, beyond the TM1 kink (at G101) seen in E2 structures10,11 (Fig. 4b and Supplementary Figs. 1,2). $MTSET^+$-accessible TM1 positions G101, F102, and L106 (Figs. 3,4) correspond to residues (rat Na^+,K^+-ATPase α1 G94, F95, and L99) important in Na^+ and K^+ binding and occlusion in E2 conformations25,26, with L99 (here L106) in particular26 cooperating with E329 (here E336) to lock exit or entry at site II. The equivalent SERCA TM1 region appears to gate cytoplasmic access for Ca^{2+} ions8,10,11.

We found no sign of reaction of 1 mM $MTSET^+$ at any of 20 contiguous TM5 positions (Fig. 2), even though the E788-equivalent TM5 residue appears accessible from the extracytoplasmic side in the open12 SERCA E2·BeF_3^- structure (Supplementary Fig. 6), and residues equivalent to S784, N785, and E788 help coordinate Rb^+ at site I in the occluded E2·MgF_4^{2-} Na^+,K^+ pump when both gates are shut21. Given that $MTSET^+$ reaction at many nearby positions altered pump-channel current (Fig. 4), it is unlikely that TM5 sites reacted without modifying current. Although we cannot rule out that distortion of the Na^+,K^+-ATPase ion pathway by palytoxin made TM5 residues inaccessible, this seems unlikely for several reasons. First, palytoxin action can be readily reversed, and repeated, on the same population of Na^+,K^+ pumps3. Second, the gates to the ion pathway through palytoxin-bound pump-channels still respond to the Na^+,K^+ pumps' physiological ligands3. Third, positions as deep as the pathway narrowing are accessible to $MTSET^+$ without palytoxin (Supplementary Fig. 3). Fourth, blockers of access channels to ion-binding sites in unmodified Na^+,K^+ pumps similarly impede cation movement in palytoxin-bound pumps23. Fifth, $MTSET^+$-accessible positions in palytoxin-bound pump-channels map reasonably onto unmodified pump structures (Fig. 4a,b, Supplementary Figs. 1,2; cf. refs. 5,16,17) and include sites expected to interact with transported ions19-21,25,26. We conclude that unfavourable geometry precluded reactivity of $MTSET^+$ with TM5 positions at site I because they do not lie on the principal ion pathway. This is consistent with little apparent influence of the side-chain charge of site-I residues E778 and D817 on cation selectivity of Na^+,K^+ pump-channels5. It is also consistent with very slow reaction of E788C with a smaller reagent, $MTSMT^+$ (1-trimethylammonium-methyl-methanethiosulphonate; Supplementary Fig. 7); similarly small $MTSEA^+$ (cf. ref. 15) is unreliable as it is membrane permeant and slowly reacts with Na^+,K^+ pumps lacking engineered cysteines (Supplementary Fig. 7).

That ~6-Å wide × ~12-Å long $MTSET^+$, $MTSES^-$, and MTSACE pass through palytoxin-bound Na^+,K^+ pump-channels corroborates the findings that these channels conduct N-methyl-D-glucamine ions (diameter ≥7 Å) only ~50 fold more slowly than Na^+ ions22, and that their measured27 Na^+ flux ratio exponent28 is ~1.0, implying little interaction between Na^+ ions in a queue along the principal pathway that passes through site II. Occupancy by a second Na^+ ion of site I, off the main pathway but linked to it via a connection narrow enough to preclude reactivity with $MTSET^+$, could account for suggested average pump-channel occupancy by two Na^+ ions23. In SERCA, lock-in of a Ca^{2+} ion in site I by binding of the second Ca^{2+} ion29 at site II, and sequential release of the two Ca^{2+} ions30, are similarly consistent with transported ions negotiating a single common pathway from the cytoplasm to the ion-binding sites in E1 states, and from those sites to the reticulum lumen

Author Manuscript Author Manuscript Author Manuscript Author Manuscript

during release in the E2P state. This snapshot of an ion pathway right through the Na^+,K^+ pump affords a structural basis for understanding cation translocation in P-type pumps.

Methods Summary

Ouabain- and MTS-insensitive *Xenopus* Na^+,K^+ pumps

Xenopus Na^+,K^+ pumps were made insensitive to ouabain and extracellular MTS reagents by the mutation C113Y (ref. 24) in *Xenopus* Na^+,K^+-ATPase α1 subunits as described18. Single cysteines were introduced into C113Y Na^+,K^+-ATPase α1 by PCR. cDNA in *pSD5* vector was transcribed *in vitro*. *Xenopus* oocytes were injected with a 50 nl mixture of 5 ng of *Xenopus* β3 and 15 ng of mutated *Xenopus* α1 cRNAs, and incubated at 18 °C for 1-3 days.

Current recordings and analysis

Currents were recorded in outside-out excised patches at 22-24 °C as described5,18. Internal (pipette) solution contained (in mM): 125 NaOH, 100 sulphamic acid, 20 HCl, 10 HEPES, 1 EGTA, 1 $MgCl_2$ and 5 MgATP (pH 7.4). External solution contained (mM): 125 NaOH or TMA-OH, 125 sulphamic acid, 10 HEPES, 5 $BaCl_2$, 0.5 $CaCl_2$ and 1 $MgCl_2$ (pH 7.6), plus 100 μM ouabain. Palytoxin (Wako Pure Chemical Industries Ltd., Osaka, Japan) was added (from 100 μM aqueous stock solution) at 50 nM, with 0.001% bovine serum albumin and 1 mM Na-borate. MTS reagents (Toronto Research Biochemicals, North York, ON, Canada) were added from ice-cold 100 mM aqueous stock solutions immediately before use, and were refreshed at 1.5-min intervals to maintain reactivity during prolonged (≥ 2 min) applications4. Alteration of palytoxin-induced current by MTS reagents was calculated as: % inhibition of $I_{palytoxin}$ = 100 * (1 - I_{after}/I_{before}), where I_{after} represents steady palytoxin-induced current at -50 mV after MTS reagent application, and I_{before} that just before. Data are given as mean ± s.e.m.

Model building

The *Xenopus* Na^+,K^+-ATPase α1 subunit homology model was built from the Ca^{2+}-ATPase E2·BeF_3^- structure (ref. 12; PDB code 3B9B) using SWISS-MODEL (http://swissmodel.expasy.org) as described5. Structural figures were prepared with PyMOL version 0.97 (http://www.pymol.org).

Supplementary Material

Refer to Web version on PubMed Central for supplementary material.

Acknowledgments

We thank Nazim Fataliev for molecular biological support, the late R.F. Rakowski for cDNAs encoding *Xenopus* α1 and β3 Na^+,K^+-ATPase subunits, and P. Nissen, B. Vilsen, and J.V. Møller for providing atomic coordinates before their publication. The work was supported by a grant from the NIH (to D.C.G) and a fellowship from the Vicente Trust (to P.A.); N.R. is presently a Jane Coffin Fund Fellow. We dedicate this paper to the memory of our colleague R.F. Rakowski.

Author Manuscript Author Manuscript Author Manuscript Author Manuscript

References

1. Läuger, P. Electrogenic Ion Pumps. Sinauer; Sunderland, MA: 1991.
2. Scheiner-Bobis G, Meyer zu Heringdorf D, Christ M, Habermann E. Palytoxin induces K^+ efflux from yeast cells expressing the mammalian sodium pump. Mol Pharmacol. 1994; 45:1132–1136. [PubMed: 7912814]
3. Artigas P, Gadsby DC. Na^+/K^+-pump ligands modulate gating of palytoxin-induced ion channels. Proc Natl Acad Sci USA. 2003; 100:501–505. [PubMed: 12518045]
4. Karlin A, Akabas MH. Substituted-cysteine accessibility method. Methods Enzymol. 1998; 293:123–145. [PubMed: 9711606]
5. Reyes N, Gadsby DC. Ion Permeation through the Na^+,K^+-ATPase. Nature. 2006; 443:470–474. [PubMed: 17006516]
6. Toyoshima C, Nomura H, Tsuda T. Lumenal gating mechanism revealed in calcium pump crystal structures with phosphate analogues. Nature. 2004; 432:361–368. [PubMed: 15448704]
7. Toyoshima C, Nakasako M, Nomura H, Ogawa H. Crystal structure of the calcium pump of sarcoplasmic reticulum at 2.6 Å resolution. Nature. 2000; 405:647–655. [PubMed: 10864315]
8. Toyoshima C, Nomura H. Structural changes in the calcium pump accompanying the dissociation of calcium. Nature. 2002; 418:605–611. [PubMed: 12167852]
9. Olesen C, et al. Dephosphorylation of the calcium pump coupled to counterion occlusion. Science. 2004; 306:2251–2255. [PubMed: 15618517]
10. Sørensen TLM, Møller JV, Nissen P. Phosphoryl transfer and calcium ion occlusion in the calcium pump. Science. 2004; 304:1672–1675. [PubMed: 15192230]
11. Toyoshima C, Mizutani T. Crystal structure of the calcium pump with a bound ATP analogue. Nature. 2004; 430:529–535. [PubMed: 15229613]
12. Olesen C, et al. The structural basis of calcium transport by the calcium pump. Nature. 2007; 450:1036–1042. [PubMed: 18075584]
13. Toyoshima C, et al. How processing of aspartylphosphate is coupled to luminal gating of the ion pathway in the calcium pump. Proc Natl Acad Sci USA. 2007; 104:19831–19836. [PubMed: 18077416]
14. Sakmann, B.; Neher, E. Single-Channel Recording. Plenum; New York: 1995.
15. Guennoun S, Horisberger JD. Structure of the 5th transmembrane segment of the Na,K-ATPase α subunit: a cysteine-scanning mutagenesis study. FEBS Lett. 2000; 482:144–148. [PubMed: 11018538]
16. Guennoun S, Horisberger JD. Cysteine-scanning mutagenesis study of the sixth transmembrane segment of the Na,K-ATPase α subunit. FEBS Lett. 2002; 513:277–281. [PubMed: 11904164]
17. Horisberger JD, Kharoubi-Hess S, Guennoun S, Michielin O. The fourth transmembrane segment of the Na,K-ATPase α subunit: a systematic mutagenesis study. J Biol Chem. 2004; 279:29542–29550. [PubMed: 15123699]
18. Artigas P, Gadsby DC. Ouabain affinity determining residues lie close to the Na/K pump ion pathway. Proc Natl Acad Sci USA. 2006; 103:12613–12618. [PubMed: 16894161]
19. Nielsen JM, Pedersen PA, Karlish SJ, Jorgensen PL. Importance of intramembrane carboxylic acids for occlusion of K^+ ions at equilibrium in renal Na,K-ATPase. Biochemistry. 1998; 37:1961–1968. [PubMed: 9485323]
20. Ogawa H, Toyoshima C. Homology modeling of the cation binding sites of Na^+K^+-ATPase. Proc Natl Acad Sci USA. 2002; 99:15977–15982. [PubMed: 12461183]
21. Morth JP, et al. Crystal structure of the sodium-potassium pump. Nature. 2007; 450:1043–1049. [PubMed: 18075585]
22. Artigas P, Gadsby DC. Large diameter of palytoxin-induced Na/K pump channels and modulation of palytoxin interaction by Na/K pump ligands. J Gen Physiol. 2004; 123:357–376. [PubMed: 15024043]
23. Harmel N, Apell HJ. Palytoxin-induced effects on partial reactions of the Na,K-ATPase. J Gen Physiol. 2006; 128:103–118. [PubMed: 16801384]

Author Manuscript Author Manuscript Author Manuscript Author Manuscript

24. Canessa CM, Horisberger JD, Louvard D, Rossier BC. Mutation of a cysteine in the first transmembrane segment of Na,K-ATPase α subunit confers ouabain resistance. EMBO J. 1992; 11:1681–1687. [PubMed: 1316269]

25. Einholm AP, Toustrup-Jensen M, Andersen JP, Vilsen B. Mutation of Gly-94 in transmembrane segment M1 of Na^+,K^+-ATPase interferes with Na^+ and K^+ binding in E_2P conformation. Proc Natl Acad Sci USA. 2005; 102:11254–11259. [PubMed: 16049100]

26. Einholm AP, Andersen JP, Vilsen B. Importance of Leu^{99} in transmembrane segment M1 of the Na^+,K^+-ATPase in the binding and occlusion of K^+ J Biol Chem. 2007; 282:23854–23866. [PubMed: 17553789]

27. Rakowski RF, et al. Sodium flux ratio in Na/K pump-channels opened by palytoxin. J Gen Physiol. 2007; 130:41–54. [PubMed: 17562821]

28. Hodgkin AL, Keynes RD. The potassium permeability of a giant nerve fibre. J Physiol. 1955; 128:61–88. [PubMed: 14368575]

29. Zhang Z, Lewis D, Strock C, Inesi G. Detailed characterization of the cooperative mechanism of Ca^{2+} binding and catalytic activation in the Ca^{2+} transport (SERCA) ATPase. Biochemistry. 2000; 39:8758–8767. [PubMed: 10913287]

30. Inesi G. Sequential mechanism of calcium binding and translocation in sarcoplasmic reticulum adenosine triphosphatase. J Biol Chem. 1987; 262:16338–16342. [PubMed: 2960677]

Author Manuscript Author Manuscript Author Manuscript Author Manuscript

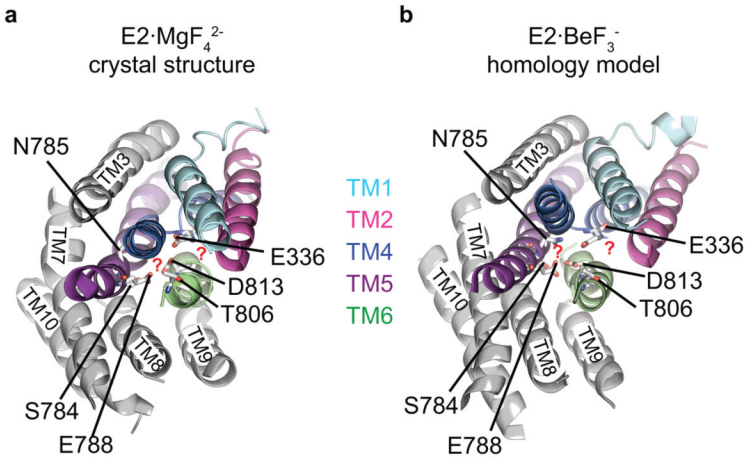

Figure 1. Alternative routes for ions through the Na^+,K^+-ATPase transmembrane domain

Extracellular views of the 10 transmembrane (TM) helices of **a**, the Na^+,K^+-ATPase $E2{\cdot}MgF_4^{2-}$ crystal structure21 (PDB 3B8E), and **b**, a homology model of the Na^+,K^+-ATPase based on the SERCA $E2{\cdot}BeF_3^-$ structure12 (PDB 3B9B). Helices are coloured grey except TM1 (pale blue), TM2 (magenta), TM4 (blue), TM5 (purple) and TM6 (green). Red question marks label two possible ion pathways: one between TM5, TM4, and TM6, and the other between TM4, TM1, TM2, and TM6. Key residues in these pathways are labelled.

Author Manuscript Author Manuscript Author Manuscript Author Manuscript

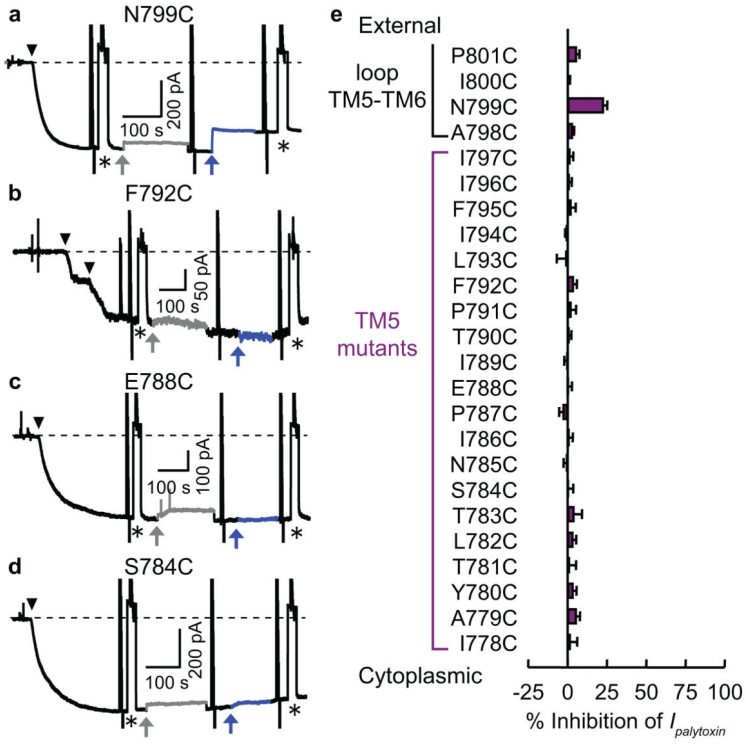

Figure 2. Effects of MTSET$^+$ on current through palytoxin-bound Na$^+$,K$^+$ pump-channels with cysteines in TM5 or TM5-TM6 loop

a-d, Current at -50 mV in outside-out patches exposed to symmetrical Na$^+$ concentrations. Application of 50 nM palytoxin (black arrowheads) generated inward (negative) current, $I_{palytoxin}$ (dashed line marks zero total membrane current). Temporary substitution (asterisk) of less permeant TMA$^+$ (tetramethylammonium) for external Na$^+$ monitored patch integrity. Application of 10 mM dithiothreitol (grey arrows, grey traces) caused a small, reversible, poorly understood current decrease. Then, 1 mM MTSET$^+$ (blue arrows, blue traces) was applied until the current became steady. **e**, Summary of mean (± s.e.m., n=3-6 patches) % inhibition of $I_{palytoxin}$ by 1 mM MTSET$^+$ at -50 mV for each single-cysteine mutant.

Author Manuscript Author Manuscript Author Manuscript Author Manuscript

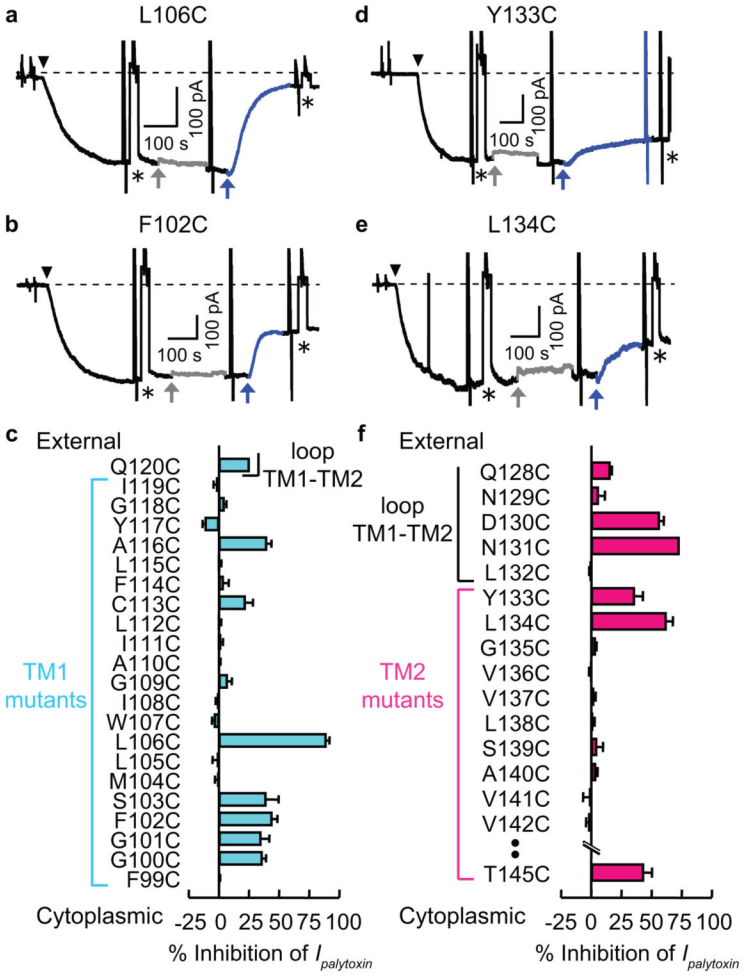

Figure 3. Effects of MTSET$^+$ on current through palytoxin-bound Na$^+$,K$^+$ pump-channels with cysteines in TM1, TM2, or TM1-TM2 loop

a, b, d, e, Representative current recordings in outside-out patches under same conditions, and with applications of palytoxin, TMA$^+$, dithiothreitol, and MTSET$^+$, as in Fig. 2. **c, f,** Summary of % inhibition of $I_{palytoxin}$ by 1 mM MTSET$^+$ at -50 mV for each single-cysteine mutant, given as mean ± s.e.m. (n=3-11 patches, except for Q120C [n=2] and N131C [n=1], both previously shown18 to be MTSET$^+$-accessible). C113C indicates data from wild type, ouabain-sensitive, *Xenopus* Na$^+$,K$^+$ pumps tested (in the absence of ouabain) in patches from non-injected control oocytes.

Author Manuscript Author Manuscript Author Manuscript Author Manuscript

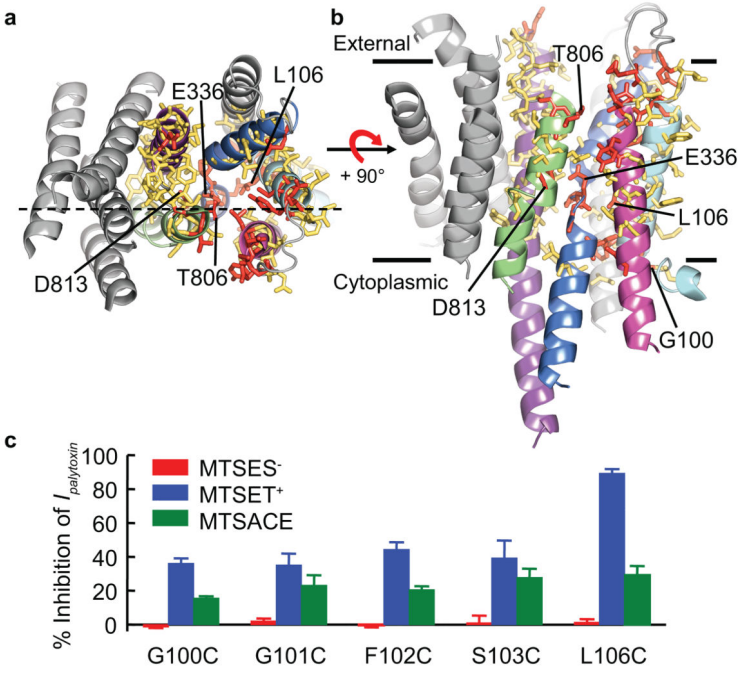

Figure 4. Structural model and characteristics of ion pathway through the palytoxin-bound Na^+,K^+-ATPase

Results (including reactive and non-responsive positions from ref. 5) mapped onto a homology model of the Na^+,K^+-ATPase TM domain (helices coloured as in Fig. 1) based on the SERCA E2·BeF_3^- structure12, viewed from the extracellular surface (**a**) or from the membrane plane (**b**). Dashed line in **a** indicates plane of cut in Supplementary Fig. 2a. Red sticks mark reactive positions ($I_{palytoxin}$ altered >10% by $MTSET^+$), and yellow sticks mark non-responsive positions. Reaction rate constants for $MTSET^+$ declined from ≥104 $M^{-1}s^{-1}$ for superficial positions to ≥10 $M^{-1}s^{-1}$ for deep positions (Supplementary Fig. 8). **c,** Accessibility of cysteines beyond the cation selectivity filter depends on charge of MTS reagent; summary of mean % inhibition (± s.e.m., n=3-8 patches) of $I_{palytoxin}$ at -50 mV by ~2.5-min applications (all 1 mM) of $MTSES^-$ (red bars), $MTSET^+$ (blue bars), or MTSACE (green bars).